

Fabrication of Flexible Microfluidic Strain Sensor by Laser Micromachining for Hand Motion Tracking

Khairul Fikri Tamrin, Nurul Amirah Khalid, and Andrew Ragai Henry Rigit

Abstract—Various types of strain sensors have been developed for providing reliable monitoring of human health. Microfluidic strain sensors is favourable for such an application due to its outstanding performance under a variety of three-dimensional deformations on the basis of elastic channel deformation. In this study, we report for the first time laser-machined micro-channels on fabricated epoxy substrate. Fabrication of flexible microfluidic sensor using soft clear epoxy is investigated. A ratio of 100:30 of epoxy resin-to-hardener results in a flexible and elastic epoxy layer. Laser micromachining (ablation) technique at varying parameters is conducted using Taguchi Experimental Design. Low number of passes for both kerf depth and kerf width gives an optimum response, while laser power and laser cutting speed differs for kerf width and kerf depth. Microstructure imaging is carried out using scanning electron microscopy for heat-affected zone examination.

Index Terms—Microfluidic, strain sensor, laser, micromachining, motion, tracking, flexible, wearable.

I. INTRODUCTION

Emerging technologies and innovation in wearable sensors have paved the ways for continuous monitoring of human's health and motion. These wearable sensors allow individuals to closely monitor vital signs (e.g., heartbeat and brain activity) and provide feedback on their health status. Robust tactile sensing capabilities on curved surfaces are often required in the applications of robotics and synthetic fingertip [1]. Due to the irregular shape of human's anatomy, development and fabrication of flexible and stretchable sensors have been continuously researched using silicon and polymer. Elastomer is a natural or synthetic polymer and has an elastic property making it the right material for flexible sensors fabrication. Various elastomers have been used which include polydimethylsiloxane (PDMS), EcoFlex™ and rubber.

Wong *et al.* [1] demonstrated a fabrication of flexible, capacitive, microfluidic sensor for normal force sensing. A flexible elastomer (used to reciprocate the properties of human skin) and a liquid metal (serves as flexible plates for the capacitive sensing units) were used to fabricate the capacitive, microfluidic sensor containing four layers of

PDMS. Pang *et al.* [2] used a reversible interlocking of nano-fibres to fabricate a flexible and highly sensitive strain-gauge sensor in which claimed to be able to distinguish numerous 'skin-like' mechanical loadings using metal-coated, high-aspect-ratio (AR) polyurethane-based nano-fibres.

Microfluidics deal with the flow of liquids inside micro meter-sized channels. Whilst, microfluidic sensors are sensors with embedded micro-channels, and usually filled with a specific conductive liquid. When the microfluidic sensor elongates due to applied stress, the geometry of the sensor will be affected resulting in the change in resistance of the (liquid) sensor. In this way, a correlation can be obtained between resistance and motion.

Casting is one of the most commonly used methods to fabricate microfluidic sensor. A mould master with the desired shape of the sensor will first be created [3]. This mould master contains the desired geometry as well as the desired micro-channel pattern. Flexible material such as rubber or latex will be poured onto the mould master to cover the template and finally heat treated. This method is time-consuming as the thermal treatment alone took approximately 10 hours to be completed. Other method such as hot-embossing is only suitable for a specific substrate only.

In view of this, laser micromachining offers some crucial benefit over other more-established micro-fabrication methods due to its low-cost operation and rapid fabrication [4]-[6]. Suriano *et al.* [7] performed a thorough study of the properties of femtosecond laser-ablated polymer surfaces for microfluidic channel fabrication. Several thermoplastic polymers such as PMMA, cyclic olefin polymer (COP) and polystyrene (PS) which were commonly used for microfluidics were studied and different characterization techniques were applied to investigate the degradation mechanisms and surface properties following laser ablation.

Teixidor *et al.* [8] conducted an experiment involving the outcome of nanosecond laser processing parameters on depth and width of micro-channels fabricated from PMMA polymer. Polymers are said to display a strong absorption in UV and deep infrared (IR) wavelengths. However, they have weak absorption at visible and near-infrared spectra. This leads to the ablation process to become a multiplex mixture of photo-chemical and photo-thermal processes.

Rahimi *et al.* [9] demonstrated the application of direct laser carbonization to fabricate high-performance stretchable electrochemical pH sensors for wearable point-of-care applications. Polyimide (PI) sheets, Eco-flex, proton-selective polymer and polyaniline (PANI) were the materials used in the experiment. Fabrication includes

Manuscript received October 29, 2019; revised March 12, 2020. This work was supported by the Ministry of Higher Education Malaysia with Grant no. F02/FRGS/1619/2017.

Khairul Fikri Tamrin, Nurul Amirah Khalid, and Andrew Ragai Henry Rigit are with the Department of Mechanical and Manufacturing Engineering, Faculty of Engineering, Universiti Malaysia Sarawak 94300 Kota Samarahan, Sarawak, Malaysia (e-mail: tkfikri@unimas.my, arigit@unimas.my).

incorporating irreversible bonding of PI to an Eco-flex substrate followed by laser carbonization and micro-machining. This omits the need for photolithographic micro-patterning and nano-material deposition. Highly porous and conductive carbon micro/nano structures were generated through laser ablation of PI.

Liao *et al.* [10] demonstrated a fast fabrication of multiplex three-dimensional micro-channel systems using femtosecond laser direct writing. This method can solve the problems where it can fabricate micro-channels with nearly limitless lengths and inconsistent geometries. For this study, they used high-silica mesoporous glass as substrate and a femtosecond laser micromachining system. Interestingly, fabrication by femtosecond laser direct writing led to smoother transition and lower flow resistance.

It is noted that the use of powerful and ultrashort lasers for micromachining of microfluidics is fairly wide. The primary objective of this paper is to investigate the application of an inexpensive low-power CO₂ laser for the fabrication of microchannels on epoxy substrate. The methodology is described in the following section.

II. METHODOLOGY

Elasticity of soft clear epoxy were investigated in this study due to its availability and flexibility. Its mechanical properties are listed in Table I. As shown in Fig. 1, the microfluidic sensor consists of two epoxy layers. The first layer (or the bottom layer) was ablated via laser micromachining method in order to fabricate the desired micro-channels. The second epoxy layer of a similar dimension was sealed onto the first layer to complete the fabrication of flexible microfluidic sensor.

TABLE I: MATERIAL PROPERTIES OF EPOXY [11]

| Property | Epoxy |
|----------------------------------|---------------|
| Viscosity at 25 °C μ (cP) | 12000 – 13000 |
| Density (g cm ⁻³) | 1.16 |
| Heat distortion temperature (°C) | 50 |
| Modulus of elasticity, E (GPa) | 5 |
| Flexural strength (MPa) | 60 |
| Tensile strength (MPa) | 73 |
| Maximum elongation (%) | 4 |

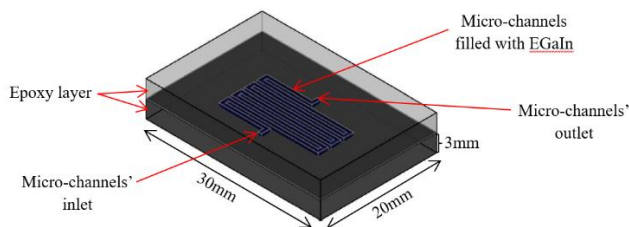


Fig. 1. Proposed CAD design of a microfluidic sensor.

Two sets of experiments were carried out to obtain the optimum epoxy resin-to-hardener (R:H) ratio which would result in a flexible and elastic microfluidic sensor. For the first set of experiment, four samples of different ratio were made, and each was labelled as A (100:10), B (100:20), C (100:30) and D (100:45), as depicted in Fig. 2. The samples were then left to cure for 24 hours. Sample A did not cure within the specified 24 hours period. It still did not cure even

after 72 hours, characterized by sticky texture similar to the condition when the mixed epoxy is poured into the mould. Samples B, C and D completely cured within the 24 hours period. Sample B is flexible but it is not elastic. After stretching, the sample was completely torn apart. The hardener ratio for sample B was not enough to produce a flexible and elastic epoxy. Sample D also completely cured but it was really hard, not flexible and obviously not elastic. Accordingly, this study shows that composition of more than 45% hardener would produce inflexible microfluidics. Sample C gives the best result out of the four samples. After completely cured, it was found out that sample C is flexible and elastic when it was stretched out, both lateral and longitudinally.

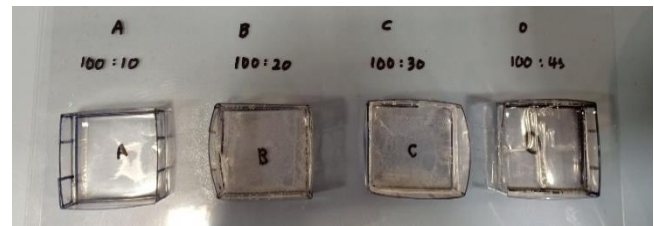


Fig. 2. First set of epoxy resin-to-hardener ratio experiment.

The second set of experiment consists of three samples, labelled as C1 (100:25), C2 (100:30) and C3 (100:35) as shown in Fig. 3. All three sample were completely cured in 24 hours. Sample C1 however, does not possess flexible and elastic characteristic as desired. Sample C2 and C3 were both flexible and elastic. Sample C3 was slightly hard compared to sample C2. After both of the experiments were carried out, it was decided that sample C from the first experiment and sample C2 from the second experiment with a ratio of 100:30 gives the optimum result in terms of flexibility and elasticity.

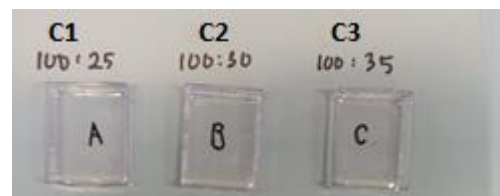


Fig. 3. Second set of epoxy resin-to-hardener ratio experiment.

TABLE II: LASER PROCESS PARAMETERS

| Factor | Variable parameters | Level | | |
|--------|------------------------------|-------|------|------|
| | | 1 | 2 | 3 |
| A | Laser power (%) | 20 | 25 | 30 |
| B | Laser cutting speed (mm/min) | 3000 | 3500 | 4000 |
| C | Number of passes | 2 | 4 | 6 |

To fabricate the micro-channels, the first epoxy layer was ablated using a 40 W CO₂ laser (FABOOL). The distance between laser focusing lens and surface of the material is 50.8 mm. The ablation was done continuously from the inlet all the way to the outlet with different parameters as listed in Table II. This was done in order to obtain a constant shape of micro-channels. Taguchi Experimental Design was used in this experiment in order to minimise the number of experiments. Effects of three input parameter on three levels (kerf width, kerf depth and surface of micro-channels) were

investigated. In comparison to our previous optimization work [12], [13], the experiments in this study were conducted using Taguchi L9 orthogonal array design with four factors at each three levels.

III. RESULTS AND DISCUSSION

Target performance measure (TPM) and noise performance measure (NPM) are the approaches employed to analyse the experimental results. TPM measures the mean output and determines the control factors that have significant effect on the mean output. Control factors can be applied to alter the mean output which corresponds to the target. Mean output can be calculated by using the following equation:

$$\bar{x} = \sum \frac{x_i}{N_i} \quad (1)$$

where \bar{x} is the mean output, x_i is the output parameter for experiment i th and N_i is the number of experiment. On the other hand, NPM is used to identify the effect of each control factor on the output parameters. In order to identify the effect of each input parameter on the output parameters, the signal-to-noise (SN) ratio is measured for each experiment. In this study, the characteristic which is the smaller-the-better was chosen to minimise the performance characteristics. SN ratio can be calculated using the following equation

$$SN \text{ ratio} = -10 \log \sum_{u=1}^{N_i} \frac{y_u^2}{N_i} \quad (2)$$

where y_u is the observed data and u is the experiment number. Table III shows the responses for all 27 experimental runs. TPM and NPM analyses for all 27 runs were evaluated by ANOVA test. ANOVA is used to detect deviation among the mean values of observation groups [14]. In order to conduct ANOVA test, Minitab 18 software was used to calculate Taguchi design and percentage contribution of each factor.

TABLE III: TAGUCHI DESIGN OF EXPERIMENT AND RESPONSE RESULTS

| Exp. | Factor | | | Response | |
|------|--------|---|---|-----------------|-----------------|
| | A | B | C | Kerf depth (mm) | Kerf width (mm) |
| 1 | 1 | 1 | 1 | 0.584 | 0.444 |
| 2 | 1 | 1 | 2 | 0.755 | 0.411 |
| 3 | 1 | 1 | 3 | 0.888 | 0.428 |
| 4 | 1 | 2 | 1 | 0.389 | 0.442 |
| 5 | 1 | 2 | 2 | 0.853 | 0.398 |
| 6 | 1 | 2 | 3 | 0.919 | 0.469 |
| 7 | 1 | 3 | 1 | 0.280 | 0.442 |
| 8 | 1 | 3 | 2 | 0.521 | 0.466 |
| 9 | 1 | 3 | 3 | 0.724 | 0.483 |
| 10 | 2 | 1 | 1 | 0.455 | 0.441 |
| 11 | 2 | 1 | 2 | 0.510 | 0.457 |
| 12 | 2 | 1 | 3 | 0.867 | 0.468 |
| 13 | 2 | 2 | 1 | 0.346 | 0.446 |
| 14 | 2 | 2 | 2 | 0.552 | 0.450 |
| 15 | 2 | 2 | 3 | 0.848 | 0.499 |
| 16 | 2 | 3 | 1 | 0.260 | 0.439 |
| 17 | 2 | 3 | 2 | 0.559 | 0.468 |
| 18 | 2 | 3 | 3 | 0.779 | 0.502 |
| 19 | 3 | 1 | 1 | 0.448 | 0.455 |
| 20 | 3 | 1 | 2 | 0.788 | 0.457 |
| 21 | 3 | 1 | 3 | 1.058 | 0.466 |
| 22 | 3 | 2 | 1 | 0.381 | 0.455 |
| 23 | 3 | 2 | 2 | 0.661 | 0.466 |
| 24 | 3 | 2 | 3 | 0.888 | 0.491 |
| 25 | 3 | 3 | 1 | 0.353 | 0.466 |
| 26 | 3 | 3 | 2 | 0.642 | 0.479 |
| 27 | 3 | 3 | 3 | 0.869 | 0.488 |

A. Kerf Width

Percentage of contribution of each control factor to the micro-channel's kerf width on TPM and NPM are shown in Table IV. For the TPM analysis, the ranking for percentage contribution for all three control factors in decreasing order are number of passes (30.68%), laser power (22.73%) and laser cutting speed (15.26%). On the other hand, the percentage contribution ranking for NPM analysis is number of passes (29.11%), laser power (23.39%) and laser cutting speed (14.83%). From both analyses, the selected optimum levels are the same which is A1B1C1.

TABLE IV: TPM AND NPM ANALYSES WITH PERCENTAGE CONTRIBUTION OF CONTROL FACTORS ON THE MICRO-CHANNELS' KERF WIDTH

| Level | TPM | | |
|----------------|----------------|--------|--------|
| | Control factor | | |
| | A | B | C |
| 1 | 0.4426 | 0.4474 | 0.4478 |
| 2 | 0.4633 | 0.4573 | 0.4502 |
| 3 | 0.4692 | 0.4703 | 0.4771 |
| % contribution | 22.73 | 15.26 | 30.68 |
| Selected level | 1 | 1 | 1 |
| Level | NPM | | |
| | Control factor | | |
| | A | B | C |
| 1 | 7.096 | 6.992 | 6.980 |
| 2 | 6.692 | 6.812 | 6.946 |
| 3 | 6.576 | 6.559 | 6.437 |
| % contribution | 23.39 | 14.83 | 29.11 |
| Selected level | 1 | 1 | 1 |
| Optimum level | 1 | 1 | 1 |

Fig. 4 and Fig. 5 show TPM mean response and SN ratio of three different factors at three levels on micro-channels' kerf width. From these analyses it is found out that lower laser power, lower cutting speed and lower number of passes will achieve maximum consistency and gives the best efficiency of the experiment when factor A operates at level 1, factor B operates at level 1 and factor C operates at level 1.

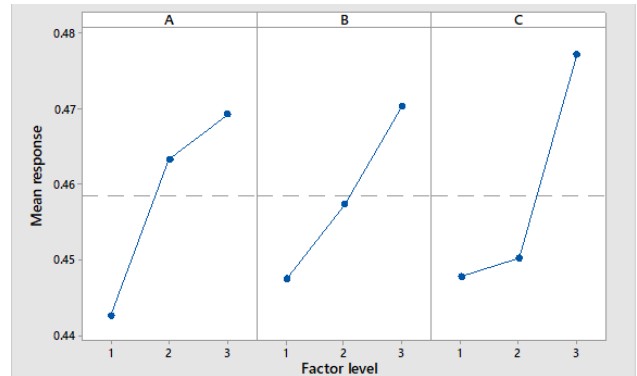


Fig. 4. TPM mean response of three different factors at three levels on micro-channels' kerf width.

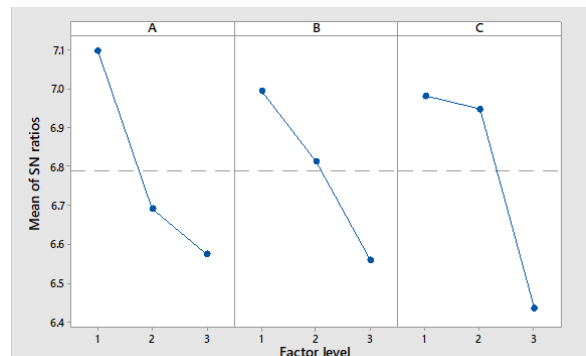


Fig. 5. SN ratio of three different factors at three levels for micro-channels' kerf width.

B. Kerf Depth

Table V shows the percentage contribution of each control factor to the kerf depth of micro-channels for both TPM and NPM analyses. For the TPM analysis, the ranking for percentage contribution for all three control factors in decreasing order are number of passes (79.46%), laser cutting speed (8.00%) and laser power (3.94). On the other hand, the percentage contribution ranking for NPM analysis is number of passes (78.44%), laser cutting speed (8.90%) and laser power (3.49%). From both analyses, the selected optimum levels are the same which is A2B3C1.

TABLE V: TPM AND NPM ANALYSES WITH PERCENTAGE CONTRIBUTION OF CONTROL FACTORS ON THE MICRO-CHANNELS' KERF DEPTH

| TPM | | | |
|----------------|----------------|--------|--------|
| Level | Control factor | | |
| | A | B | C |
| 1 | 0.6570 | 0.7059 | 0.3884 |
| 2 | 0.5751 | 0.6486 | 0.6490 |
| 3 | 0.6764 | 0.5541 | 0.8711 |
| % contribution | 3.94 | 8.00 | 79.46 |
| Selected level | 2 | 3 | 1 |
| NPM | | | |
| Level | Control factor | | |
| | A | B | C |
| 1 | 4.221 | 3.403 | 8.454 |
| 2 | 5.407 | 4.349 | 3.896 |
| 3 | 3.964 | 5.840 | 1.241 |
| % contribution | 3.49 | 8.90 | 78.44 |
| Selected level | 2 | 3 | 1 |
| Optimum level | 2 | 3 | 1 |

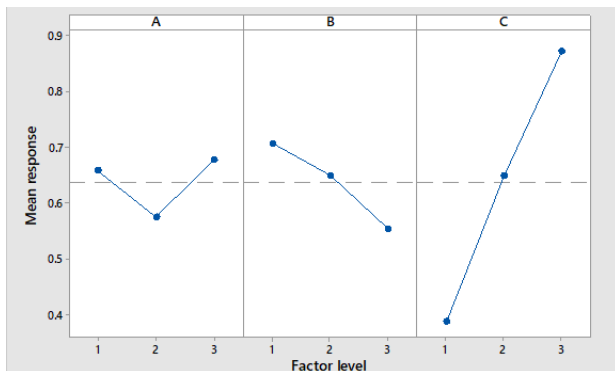


Fig. 6. SN ratio of three different factors at three levels for micro-channels' kerf depth.

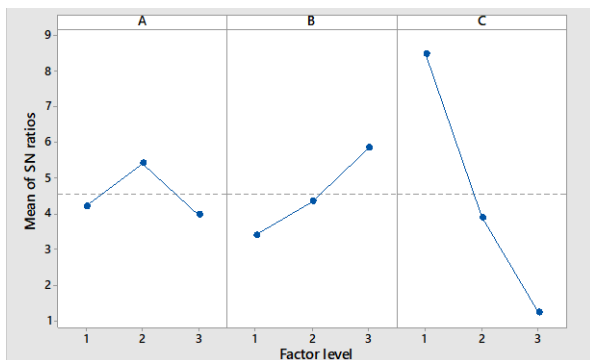


Fig. 7. SN ratio of three different factors at three levels for micro-channels' kerf depth.

Fig. 6 and Fig. 7 show TPM mean response and SN ratio of three different factors at three levels on micro-channels' kerf depth. From these analyses it is found out that higher laser power, higher cutting speed and lower number of passes will achieve maximum consistency and gives the best efficiency of the experiment when factor A operates at level 1, factor B operates at level 3 and factor C operates at level 1.

This shows that lower number of passes for both kerf depth and kerf width give an optimum response meanwhile laser power and laser cutting speed differs for kerf width and kerf depth, as evident in Fig. 8.

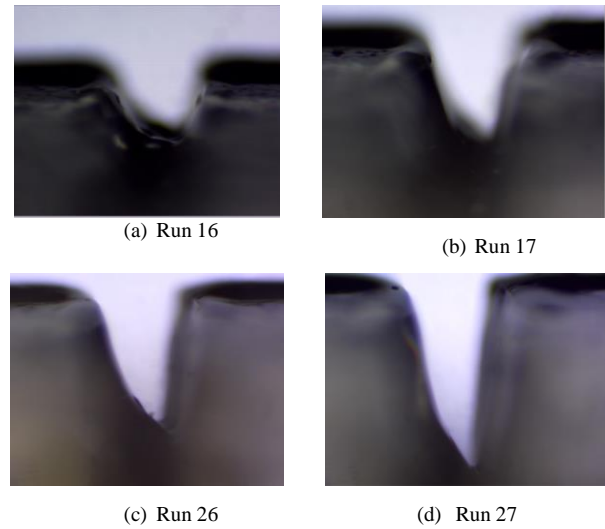


Fig. 8. Cross-sectional views of micro-channels.

Microstructure characterization of the laser processed micro-channel due to ablation of CO₂ laser for run 1 is shown in Fig. 9. The size of heat-affected zone is not consistent throughout the ablated region, characterized by resolidified epoxy region. It can also be observed that the micro-channel appears uneven and crooked. The kerf depth of the micro-channel can be seen to be uneven and not uniform. Some part can be seen to be evenly ablated (darker shade). This can be attributed to the way epoxy laser was originally fabricated, causing uneven surface of the epoxy layer which consequently results in varying stand-off distance.

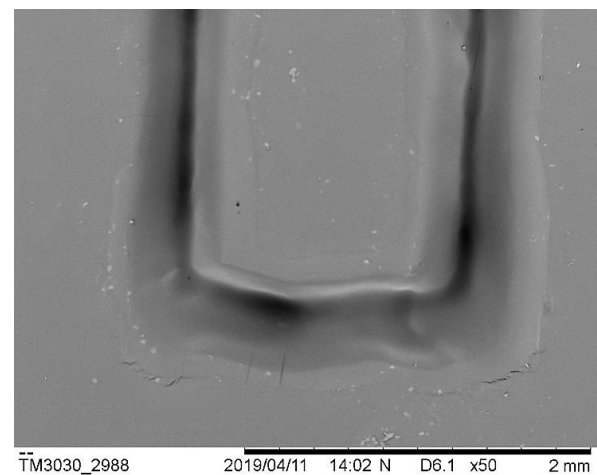


Fig. 9. SEM image of ablated micro-channel (run 1).

IV. CONCLUSION

In this paper, a flexible microfluidic strain sensor was successfully fabricated by using laser micromachining (ablation) technique using Taguchi Experimental Design method. The Taguchi L9 array method was chosen in order to determine the optimum laser process parameters. The effects of three different factors on kerf width and kerf depth

were evaluated in this study, namely laser power (20% to 30%), cutting speed (3000 mm/min to 4000 mm/min) and number of passes (2 to 6 passes). To get an optimum kerf width, low laser power, low cutting speed and low number of passes are desirable. Meanwhile, the optimum kerf depth can be obtained at medium laser power, high cutting speed and low number of passes. Future work includes injecting a conductive liquid (EGaIn) into the micro-channels for determining the relationship between three-dimensional deformation and resistivity.

CONFLICT OF INTEREST

The authors declare no conflict of interest.

AUTHOR CONTRIBUTIONS

K. F. T. designed the experiment; N. A. K conducted the experiment; K. F. T and N.A.K analyzed the data; K. F. T., N. A. K and A. R. H. R wrote the paper; all authors had approved the final version.

REFERENCES

- [1] R. D. P. Wong, J. D. Posner, and V. J. Santos, "Flexible microfluidic normal force sensor skin for tactile feedback," *Sensors and Actuators A: Physical*, vol. 179, pp. 62-69, 2012.
- [2] C. Pang *et al.*, "A flexible and highly sensitive strain-gauge sensor using reversible interlocking of nanofibres," *Nature Materials*, vol. 11, no. 9, p. 795, 2012.
- [3] F. C. Cabrera *et al.*, "Natural-rubber-based flexible microfluidic device," *Rsc Advances*, vol. 4, no. 67, p. 35467-35475, 2014.
- [4] K. Tamrin *et al.*, "Experiment and prediction of ablation depth in excimer laser micromachining of optical polymer waveguides," *Advances in Materials Science and Engineering*, 2018.
- [5] M. Harizam *et al.*, "Effect of process parameters on the laser joining of stainless steel with three-dimensional (3-D) printed polymer sheet," *Lasers in Engineering*, vol. 41, 2018.
- [6] K. F. Tamrin, S. Zakariyah, and N. Sheikh, "Multi-criteria optimization in CO₂ laser ablation of multimode polymer waveguides," *Optics and Lasers in Engineering*, vol. 75, pp. 48-56, 2015.
- [7] R. Suriano *et al.*, "Femtosecond laser ablation of polymeric substrates for the fabrication of microfluidic channels," *Applied Surface Science*, vol. 257, no. 14, pp. 6243-6250, 2011.
- [8] D. Teixidor *et al.*, "Effect of process parameters in nanosecond pulsed laser micromachining of PMMA-based microchannels at near-infrared and ultraviolet wavelengths," *The International Journal of Advanced Manufacturing Technology*, vol. 67, no. 5-8, pp. 1651-1664, 2013.
- [9] R. Rahimi *et al.*, "Highly stretchable potentiometric pH sensor fabricated via laser carbonization and machining of carbon-polyaniline composite," *ACS applied Materials & Interfaces*, vol. 9, no. 10, pp. 9015-9023, 2017.
- [10] Y. Liao *et al.*, "Rapid prototyping of three-dimensional microfluidic mixers in glass by femtosecond laser direct writing," *Lab on a Chip*, vol. 12, no. 4, pp. 746-749, 2012.

- [11] A. A. Ibrahim and M. F. Hassan, "Study the mechanical properties of epoxy resin reinforced with silica (quartz) and alumina particles," *Iraqi Journal of Mechanical and Material Engineering*, vol. 11, no. 3, pp. 486-506, 2011.
- [12] K. F. Tamrin *et al.*, "Multiple-objective optimization in precision laser cutting of different thermoplastics," *Optics and Lasers in Engineering*, vol. 67, pp. 57-65, 2015.
- [13] K. Tamrin and A. Zahrim, "Determination of optimum polymeric coagulant in palm oil mill effluent coagulation using multiple-objective optimisation on the basis of ratio analysis (MOORA)," *Environmental Science and Pollution Research*, vol. 24, no. 19, pp. 15863-15869, 2017.
- [14] N. W. Galwey, *Introduction to Mixed Modelling: Beyond Regression and Analysis of Variance*, John Wiley & Sons, 2014.

Copyright © 2020 by the authors. This is an open access article distributed under the Creative Commons Attribution License which permits unrestricted use, distribution, and reproduction in any medium, provided the original work is properly cited ([CC BY 4.0](https://creativecommons.org/licenses/by/4.0/)).



Khairul Fikri Tamrin is a senior lecturer at Universiti Malaysia Sarawak (UNIMAS). He is a chartered engineer (IMechE, UK) with research focus in laser materials processing for the applications in microfluidics, automotive, aerospace and manufacturing sectors. In addition, he had designed and developed a number of laser optical measurement techniques i.e., particle image velocimeter and digital holographic microscope for biomedical application. He has continuously published the research findings of his international collaborative research work in high impact journals.



Nurul Amirah Khalid Nurul Amirah Khalid, is a postgraduate (MEng) student in the Department of Mechanical and Manufacturing Engineering at the Universiti Malaysia Sarawak (UNIMAS). She has earned her bachelor degree with honours in mechanical and manufacturing engineering from UNIMAS. Having been involved in various projects throughout her degree years, her final year project "Development of flexible microfluidic strain sensor by laser micromachining for human motion monitoring" left the biggest impression on her as it has challenged her in every aspect possible. Currently, she is fully engaged in her master's degree project that aims to study the modal analysis of gong using finite element analysis through software such as ANSYS as a requisite to obtain the master's degree.



Andrew Ragai Henry Rigit is a professor at Faculty of Engineering, Universiti Malaysia Sarawak (UNIMAS). He is a professional engineer registered with Board of Engineers, Malaysia. His research focus is in electrohydro dynamics, fluid, discharges and plasma physics, and fluid dynamics. He received the doctor of philosophy in mechanical engineering from Imperial College London in 2004; He received the master of science in mechanical engineering from Universiti Malaysia Sarawak in 1997; He also received the bachelor of engineering in mechanical engineering from City University in 1995.